

# The Glycophospholipid-linked Folate Receptor Internalizes Folate Without Entering the Clathrin-coated Pit Endocytic Pathway

Karen G. Rothberg,\* Yunshu Ying,\* J. Fred Kolhouse,|| Barton A. Kamen,‡§ and Richard G. W. Anderson\*

Departments of \*Cell Biology and Neuroscience, ‡Pediatrics, and §Pharmacology, University of Texas Southwestern Medical Center, Dallas, Texas 75235; and ||Divisions of Hematology and Oncology, University of Colorado Health Sciences Center, Denver, Colorado 80262

**Abstract.** The folate receptor, also known as the membrane folate-binding protein, is maximally expressed on the surface of folate-depleted tissue culture cells and mediates the high affinity accumulation of 5-methyltetrahydrofolic acid in the cytoplasm of these cells. Recent evidence suggests that this receptor recycles during folate internalization and that it is anchored in the membrane by a glycosyl-phosphatidylinositol linkage. Using quantitative immunocytochem-

istry, we now show that (a) this receptor is highly clustered on the cell surface; (b) these clusters are preferentially associated with uncoated membrane invaginations rather than clathrin-coated pits; and (c) the receptor is not present in endosomes or lysosomes. This receptor appears to physically move in and out of the cell using a novel uncoated pit pathway that does not merge with the clathrin-coated pit endocytic machinery.

**O**VER 25 different membrane receptors have been identified that participate in receptor-mediated endocytosis (4, 24). Characteristically, these receptors are transmembrane glycoproteins that bind protein ligands and carry them into an endocytic system. In many cases, the receptor is recycled back to the cell surface where it participates in subsequent rounds of internalization while at the same time the ligand is transported to other intracellular compartments such as the lysosome (11). The clathrin-coated pit is the staging area for this process since it controls both receptor clustering and the formation of the endosome (3, 25).

The folate receptor, also known as the membrane folate binding protein, is a membrane protein that has some features of a receptor that is involved in receptor-mediated endocytosis. The molecule is maximally expressed on the surface of folate-depleted tissue culture cells and is responsible for the high affinity accumulation of 5-methyltetrahydrofolic acid (5-CH<sub>3</sub>FH<sub>4</sub>)<sup>1</sup> in the cytoplasm of these cells (8, 26–28, 35). In MA104 cells, the surface membrane has two equal sets of receptors: one set is exposed to the extracellular environment, and the other is not accessible to this space. Several lines of evidence suggest that ordinarily the two sets of receptors completely exchange with each other once every hour (27, 28). Kinetic studies have shown that this exchange reaction results in the delivery of bound 5-methyltetrahydrofolic acid to the cytoplasm (28) and that delivery is blocked by

ionophores that disrupt proton gradients (27). Therefore, the folate receptor internalizes 5-CH<sub>3</sub>FH<sub>4</sub> and recycles.

Other information about the folate receptor is not consistent with the receptor-mediated endocytosis paradigm. Recently, we showed (30) that this receptor is anchored in the membrane by a glycosyl-phosphatidylinositol (GPI) linkage. Although a variety of membrane proteins are membrane anchored in this manner (19, 33), none of these proteins have been found to be involved in receptor-mediated endocytosis. There is good experimental evidence that the membrane-spanning region together with the cytoplasmic tail (5, 16, 17, 31, 42) of receptors that participate in receptor-mediated endocytosis are the domains that control receptor internalization. Also, Thy-1 is a GPI-linked protein (32) that has been found to be excluded from clathrin-coated pits (10).

Biochemical methods have been used to dissect the pathway of 5-CH<sub>3</sub>FH<sub>4</sub> internalization in MA104 cells (26–28). Four steps in the process have been identified: (a) binding of 5-CH<sub>3</sub>FH<sub>4</sub> to externally oriented receptors; (b) movement of receptor–ligand complex into a compartment that is protected from the 5-CH<sub>3</sub>FH<sub>4</sub> releasing effects of acid treatment; (c) dissociation of 5-CH<sub>3</sub>FH<sub>4</sub> from the receptor and passage across the membrane into the cytoplasm; and (d) the addition of multiple glutamic acid residues to form a folyl-polyglutamic acid. To better understand how a membrane protein that is anchored by a GPI linkage can mediate the internalization of 5-CH<sub>3</sub>FH<sub>4</sub>, as well as recycle, we have used immunocytochemistry to map the distribution of this receptor in MA104 cells. In this cell, folate receptors are highly clustered but recycle by a pathway that does not involve clathrin-coated pits.

1. *Abbreviations used in this paper:* 5-CH<sub>3</sub>FH<sub>4</sub>, 5-methyltetrahydrofolic acid; DNP, dinitrophenol; GPI, glycophospholipid; LDL, low density lipoprotein; TNP, 2,4,6 trinitrophenol.

## Materials and Methods

### Materials

Goat anti-chicken IgG conjugated to FITC (02-24-06) and goat anti-chicken IgG (H+L) (01-24-06) were from Kirkegaard & Perry Laboratories, Inc. (Gaithersburg, MD). Goat anti-rabbit IgG conjugated to FITC (62-1811) and rabbit anti-chicken IgG conjugated to FITC (61-3111) were from Zymed Laboratories (South San Francisco, CA). Polyclonal anti-low density lipoprotein (LDL) receptor IgG (2, 6) was prepared as previously described. Monoclonal anti-dinitrophenol (DNP) IgG was from Oxford Biochemical Research (Oxford, MI). 10-nm goat anti-rabbit-gold (BC-PAG-10), 3 OD at 520 nm, was from Energy Beam Sciences (Agawan, MA). Rabbit anti-chicken IgG (H+L) (0204 0082) was from Organon Teknika-Cappel (West Chester, PA). Medium 199 with Earle's salt with (320-1150) or without (82-002) folic acid, glutamine (320-5030), trypsin-EDTA (610-5300), and penicillin/streptomycin (600-5145AE) was from Gibco Laboratories (Grand Island, NY). FCS (12-10378) was from Hazelton Research Products, Inc. (Lenexa, KS). T-75 culture flasks and 35-mm dishes were from Corning Glass Works (Corning, NY). Human lipoprotein-deficient serum ( $d > 1.215$  g/ml) was isolated from the plasma of healthy donors by ultracentrifugation (23). ITS Premix (containing insulin, transferrin, and selenium) was from Collaborative Research (Bedford, MA). Sodium sulfate (8024) was from Mallinckrodt Inc. (St. Louis, MO). Potassium carbonate (60108), sodium borohydride (71320), potassium chloride (60130), magnesium chloride (63065), paraformaldehyde (76240), and 2,4,6 trinitrophenol (TNP) (80450) were from Fluka (Ronkonkoma, NY). Tris (T-1503), Hepes (H-3375), crystalline BSA (A-7638), and Triton X-100 (T-6878) were from Sigma Chemical Co. (St. Louis, MO). Tween-20 (170-6531) was from Bio-Rad Laboratories (Richmond, CA). Sodium azide (S-227), sodium metaperiodate (S-398), and ammonium chloride (A-661) were from Fisher Scientific Co. (Fairlawn, NH). Osmium tetroxide (19110), glutaraldehyde (16300), uranyl acetate (22400), and lead citrate (17800) were from Electron Microscopy Sciences (Fort Washington, PA). Eponate (18005), dodecyl succinic anhydride (18022), nadic methyl anhydride (18032), and 2,4,6-trimethyl-aminoethyl phenol (18042) were from Pelco (Tusten, CA).

### Methods

#### ANTI-FOLATE RECEPTOR ANTIBODY

The antibody used for the studies was raised in chickens against the membrane folate-binding protein isolated from cultured KB cells (18, 29). The chicken serum was subjected to sodium sulfate precipitation to enrich for the IgG fraction (9), and this was routinely used at a concentration ranging from 17 to 42  $\mu\text{g/ml}$ . By immunoblotting, the antibody recognizes purified folate receptor isolated from human placenta as well as purified folate receptor from  $\text{CaCO}_2$  cells (data not shown). As a test for the specificity of the antibody, we have shown previously that this antibody binds weakly to mock transfected COS-1 cells, which have low amounts of folate receptor, but very strongly to COS-1 cells that have been transfected with a cDNA to the folate receptor, which express 50 times more folate receptor (30).

#### CELL CULTURE

MA104 cells, a monkey kidney epithelial cell line, and  $\text{CaCO}_2$  cells, a human intestinal carcinoma cell line, were grown continuously as a monolayer in folic acid-free medium 199 supplemented with 5% (vol/vol) FCS and 100 U/ml penicillin/streptomycin (medium A). Complete medium contained  $\sim 10$  nM folate and 0.68 mM glutamine. Cells for each experiment were set up according to a standard format. On day 0,  $2 \times 10^5$  cells were seeded into a 35-mm dish and grown for 5 d in the same medium A. When the medium was assayed for folates (26), by day 4 there was  $< 1$  nM folates, and the cells contained  $< 1$  pmol/ $10^6$  cells of folate. Some sets of cells were induced to express LDL receptors by replacing the FCS in medium A with 10% human lipoprotein-deficient serum (23). Human fibroblasts were cultured according to a standard format as previously described (23).

#### INDIRECT IMMUNOFLUORESCENCE

The sequences of antibody incubations and fixation protocols varied with the experimental procedure and are outlined in the figure legends. For incubating with unfixed cells, anti-folate receptor IgG was diluted to the indicated concentration in buffer A (folate-free medium 199, 20 mM Hepes, pH 7.4, 0.1% crystalline BSA). For incubating with fixed cells, antibodies were

diluted in buffer B (2.68 mM KCl, 1.46 mM  $\text{KH}_2\text{PO}_4$ , 8 mM  $\text{Na}_2\text{HPO}_4 \cdot 7\text{H}_2\text{O}$ , 200 mM NaCl, 0.49 mM  $\text{MgCl}_2$ , pH 7.4, 0.1% crystalline BSA). Cells were fixed with 3% formaldehyde in buffer C (buffer B minus the BSA) or 3% formaldehyde plus 3 mM TNP in buffer C and permeabilized with either 0.1% Triton X-100 or 0.1% Tween 20 in buffer C.

#### IMMUNOGOLD LABELING PROCEDURE

Cells were either labeled before fixation or first fixed, permeabilized, and labeled by the DNP/immunogold method of Pathak and Anderson (39). To localize receptors in unfixed cells, MA104 cells were incubated with anti-receptor IgG in buffer A (42  $\mu\text{g/ml}$ ) at the indicated temperature and then chilled to 4°C and incubated sequentially with unlabeled rabbit anti-chicken IgG in buffer A (25  $\mu\text{g/ml}$ ) and gold-conjugated goat anti-rabbit IgG in buffer B (1:50 dilution) all for 60 min at 4°C. Cells were extensively washed with buffer A or B between each incubation. At the end of the incubation, the cells were rinsed extensively with buffer C and then buffer D (0.1 M cacodylate, pH 7.4) and then fixed with 2% glutaraldehyde containing 5 mM  $\text{CaCl}_2$  in buffer D at 4°C. Fixed and permeabilized cells were processed as previously described (39) with the following modifications: after fixation with 3% formaldehyde plus 3 mM TNP in buffer C and aldehyde blocking, the cells were incubated with anti-receptor IgG (42  $\mu\text{g/ml}$ ) in buffer B for 60 min at 4°C, rinsed with buffer B, and then incubated with DNP-labeled goat anti-chicken IgG (20  $\mu\text{g/ml}$ ) for 60 min at 4°C. Cells were rinsed with buffer C and fixed in glutaraldehyde as described above. All cells were subsequently postfixed in 1%  $\text{OSO}_4$ , 1.5% potassium ferricyanide in buffer D at 4°C for 60 min, dehydrated in ethanol, stained en bloc with 1% uranyl acetate in 70% ethanol, further dehydrated with ethanol, propylene oxide, and embedded in Eponate.

For anti-DNP gold labeling, thin sections on nickel grids were etched for 30 min in saturated sodium metaperiodate and jet washed with water. Grids were then blocked with 1% crystalline BSA in buffer E (20 mM Tris, 200 mM NaCl, 3 mM  $\text{NaN}_3$ , pH 8.5) for 1 h at room temperature, incubated with anti-DNP (1  $\mu\text{g/ml}$ ) in buffer F (buffer E with 0.1% crystalline BSA) overnight at room temperature, and then washed twice for 5 min each with buffer F. Grids were subsequently incubated with rabbit anti-mouse IgG (5  $\mu\text{g/ml}$ ) in buffer F followed by goat anti-rabbit IgG conjugated to gold (10 nm diameter) diluted 1:50 in buffer F. After jet washing grids with distilled water, sections were stained with 4% uranyl acetate and 1% lead citrate.

#### RAPID-FREEZE, DEEP-ETCH REPLICAS

MA104 cells were chilled to 4°C, medium was replaced with ice cold buffer A containing 42  $\mu\text{g/ml}$  of anti-receptor IgG, and the cells were incubated for 1 h at 4°C. The cells were then washed, incubated for 1 h at 4°C with 25  $\mu\text{g/ml}$  of rabbit anti-chicken IgG in buffer A, washed again, and incubated with anti-rabbit IgG conjugated to gold (10 nm diameter) diluted 1:50 in buffer B. The cells were then washed and fixed with 4% glutaraldehyde in buffer C for 30 min at 4°C. The coverslip containing the labeled cells was rapidly frozen using a Cryopress freezing device (Med VAC, Inc., St. Louis, MO) and liquid nitrogen as the coolant. Samples were etched for 14 min at a stage temperature of  $-80^\circ\text{C}$  and coated with platinum and carbon using a freeze-fracture unit (model 301; Balzers, Hudson, NH) with a rotating stage set at maximum setting. The samples were coated with  $\sim 9$  Å of platinum using an electron gun at an angle of  $17^\circ$ . The replica was then reinforced with  $\approx 120$  Å of carbon using an electron gun at an angle of  $\sim 50^\circ$ . Replicas were floated free of the coverslip with 30% hydrofluoric acid and digested with Clorox for 45 s before mounting on a formvar-coated grid.

#### QUANTITATIVE ANALYSIS

**Indirect Immunofluorescence.** Photographs were prepared from three experiments to evaluate the number of anti-folate receptor clusters on the surface of MA104 cells incubated with antibody at either 4 or 37°C. Samples were coded and photographed at random with a photomicroscope III (Carl Zeiss, Inc., Thornwood, NY) using the automatic exposure system. Pictures were printed to a final magnification of 1,800 $\times$ , coded, and evaluated. Fluorescent foci in 12 regions (30  $\mu\text{m}^2$ /region) on each of 107 pictures (4°C,  $n = 53$ ; 37°C,  $n = 54$ ) were tabulated by counting the number of foci that lay within a grid overlay.

**Immunogold Labeling.** Electron microscope negatives were obtained by randomly photographing 50 regions per experimental treatment. Two separate experiments representing 200 electron micrographs were evaluated (100 for 4°C incubation and 100 for 37°C incubation). Negatives were projected

to final magnification of 90,720 $\times$  with a Slide King II lantern projector (Bessler, Linden, NJ). Surface length, number of gold particles, number of clusters (where a cluster was defined as containing more than three gold particles), number and diameter of coated and uncoated invaginations, and number and length of clusters were determined directly. Statistical evaluations were made using standard *t* test for unpaired samples.

**Replica Labeling.** To determine the area occupied by each cluster of gold particles, micrographs of replicas labeled with anti-folate IgG, rabbit anti-chicken IgG, and goat-anti rabbit conjugated to gold (10 nm) at 4 $^{\circ}$ C were printed to a final magnification of 31,688 $\times$ . The surface area occupied by each cluster of gold particles was estimated using a grid overlay. Surface area was determined on 163 clusters from immune labeled replicas.

#### OTHER PROCEDURES

Protein determinations were made by the method of Lowry et al. (34) using BSA as a standard. All electron microscopic observations and photography were made with a JEOL USA (Cranford, NJ) 100 CX electron microscope. Fluorescence photographs were made on a photomicroscope III (Carl Zeiss, Inc.) using an automatic photometer unless otherwise specified in figure legends. 5-methyl[ $^3$ H]tetrahydrofolic acid binding assays on CaCO $_2$  cells and human fibroblasts were carried out as previously described (27).

## Results

### Indirect Immunofluorescence Localization of the Folate Receptor

The antibody used in these studies was produced in chickens and directed against the human folate receptor isolated from KB cells (18, 29). This antibody binds preferentially to COS-1 cells that express a cDNA coding for the folate receptor (30). Since the MA104 cell had been used in all of our previous biochemical studies, we first examined these cells for the binding of the chicken anti-receptor IgG. Cells were incubated with 17  $\mu$ g/ml of the antibody at 4 $^{\circ}$ C, washed, and then incubated with fluorescein-labeled rabbit anti-chicken IgG. MA104 cells incubated with immune IgG (Fig. 1 *A*) had numerous punctate fluorescent dots uniformly covering the surface of the cell. Cells incubated with the nonimmune

chicken IgG (Fig. 1 *B*) were devoid of any immunofluorescence staining pattern. Since the nonimmune chicken IgG was not from the same animal that had been immunized with the KB cell folate receptor, as a control for the specificity of the antibody, cells were incubated at 4 $^{\circ}$ C with immune IgG that had been adsorbed with purified human placenta folate receptor. As shown in Fig. 1 *C*, the adsorbed antibody gave a much reduced staining pattern.

To further test the specificity of the antibody, we used the intensity of the immunofluorescence signal to assess the ability of the anti-receptor IgG to bind to three different cell lines that each express different levels of 5-methyltetrahydrofolic acid binding activity. Compared with MA104 cells (Fig. 2 *A*), the CaCO $_2$  cells (Fig. 2 *B*) had many more punctate fluorescent foci on the cell surface, which is consistent with the >10-fold higher 5-methyl[ $^3$ H]tetrahydrofolic acid binding activity that these cells express (10 pmol/10 $^6$  cells). By contrast, human fibroblasts (Fig. 2 *C*), which bind 10-fold less 5-methyl[ $^3$ H]tetrahydrofolic acid than the MA104 cells (0.08–0.12 pmol/10 $^6$  cells) and do not contain detectable levels of folate receptor mRNA (30), were devoid of any antibody staining.

Previous biochemical experiments have established that there are two populations of folate receptors: at 4 $^{\circ}$ C, one population binds 5-CH $_3$ FH $_4$  and the other is inaccessible for binding. These two populations of receptors readily exchange with each other at 37 $^{\circ}$ C (27, 28). To determine if the anti-folate receptor IgG could also distinguish between accessible and inaccessible receptors, cells were incubated with the antibody at either 4 or 37 $^{\circ}$ C and then processed for indirect immunofluorescence. A comparison of Fig. 3, *A* with *B*, shows that those cells incubated at 37 $^{\circ}$ C (Fig. 3 *B*) had considerably more punctate fluorescent foci on the cell surface than those incubated at 4 $^{\circ}$ C, which indicates that more receptors became available for antibody binding at 37 $^{\circ}$ C. By quantitative analysis (Table I), the 37 $^{\circ}$ C incubated

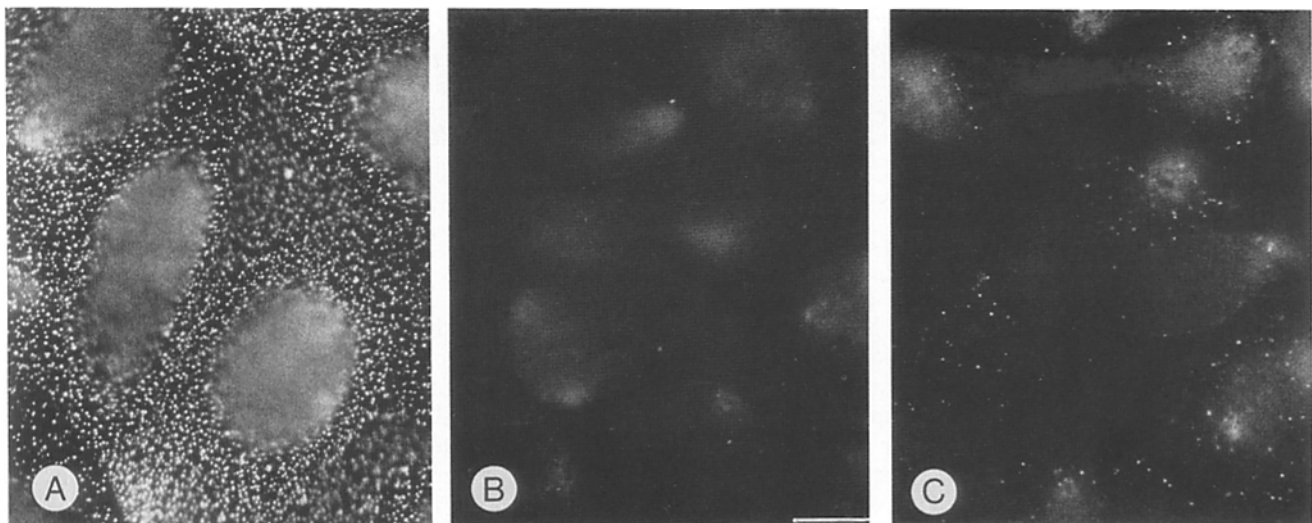


**Figure 1.** Immunofluorescence localization of anti-folate receptor IgG binding sites at 4 $^{\circ}$ C. MA104 cells were grown on coverslips, chilled to 4 $^{\circ}$ C, and incubated with 17  $\mu$ g/ml of either immune (*A*), nonimmune (*B*), or adsorbed (*C*) IgG for 60 min. Adsorbed anti-folate receptor IgG was prepared by mixing anti-folate receptor IgG (17  $\mu$ g/ml) with purified placental folate receptor (3.2  $\mu$ g/ml) and incubating overnight at 4 $^{\circ}$ C before incubating with MA104 cells at 4 $^{\circ}$ C. After the incubations, the cells were fixed and processed to localize chicken IgG. Bar, 12  $\mu$ m.

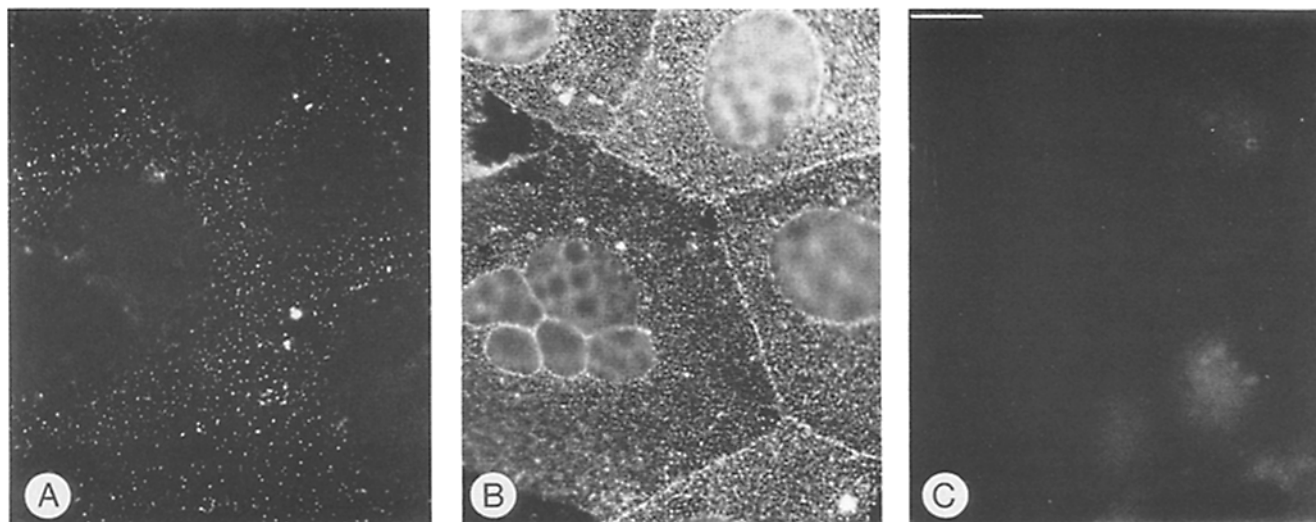


**Figure 2.** Immunofluorescence localization of anti-folate receptor IgG binding sites in MA104 cells (A), CaCO<sub>2</sub> cells (B), and human fibroblasts (C). Application of antibodies at 4°C and immunofluorescence was carried out as described in Fig. 1. To compare the fluorescence intensity among the samples, the CaCO<sub>2</sub> cells were photographed using the automatic photometer system of the microscope, and the other two sets of cells were photographed manually using the same exposure time as for the CaCO<sub>2</sub> cells. Bar, 10 μm.

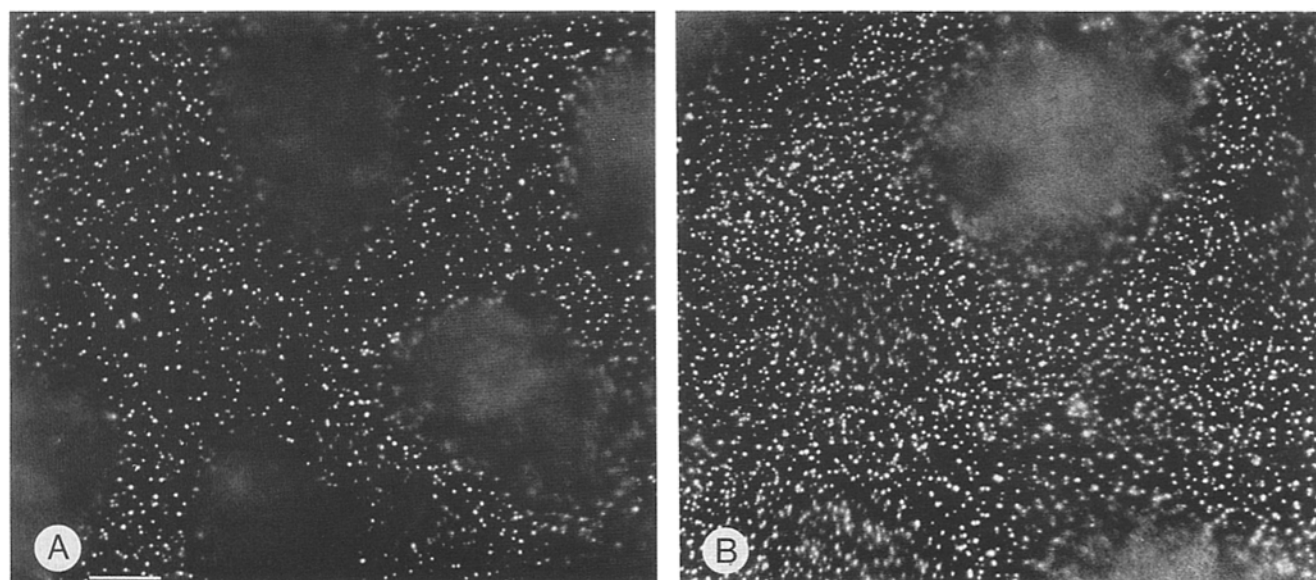


**Figure 3.** Distribution of anti-folate receptor IgG binding sites at 4°C (A) and 37°C (B). Cells were incubated at the indicated temperature with 17 μg/ml of antibody for 1 h. The cells were then washed at 4°C, fixed, and processed to localize antibody by indirect immunofluorescence. Bar, 6 μm.

cells had 1.6 times more fluorescent foci per square micrometer of cell surface than did 4°C incubated cells.

The punctate fluorescence pattern was similar to that seen for clustered receptors involved in receptor-mediated endocytosis. One test of whether a receptor is internalized by coated pits is to determine whether the receptor will deliver an anti-receptor IgG to an endocytic compartment (6, 21, 36, 37). Therefore, we incubated MA104 cells that had been induced to express LDL receptors (which are internalized by coated pits) in the presence of either anti-LDL receptor IgG (Fig. 4, A-C) or anti-folate receptor IgG (Fig. 4, D-F) at 4°C, shifted the temperature to 37°C for 30 min (Fig. 4, B,

C, E, and F), and then processed the cells to visualize either surface bound antibody (Fig. 4, A, B, D, and E) or internalized antibody (Fig. 4, C and F). There was almost a complete loss of anti-LDL receptor IgG from the surface of cells that had been shifted to 37°C (compare Fig. 4, A with B). In permeabilized cells, this antibody was found in vesicles near the nucleus (Fig. 4 C). By contrast, there was little loss of anti-folate receptor IgG from the surface of warmed cells (compare Fig. 4, D with E), and IgG was not found within intracellular vesicles (Fig. 4 F).

To determine if there were any folate receptors in an internal vacuolar compartment, MA104 cells were fixed and per-

**Table I. Number of Anti-folate Receptor IgG Clusters at 4°C vs. 37°C**

Experiment	4°C	37°C
	clusters/ $\mu\text{m}^2$	clusters/ $\mu\text{m}^2$
1	1.00 $\pm$ .03 (17)	1.52 $\pm$ .03* (18)
2	1.00 $\pm$ .03 (18)	1.69 $\pm$ .03* (19)
3	1.12 $\pm$ .04 (18)	1.81 $\pm$ .04* (18)
$\bar{x}$	1.04	1.68

MA104 cells were incubated for 1 h with 17  $\mu\text{g}/\text{ml}$  of anti-receptor IgG either at 4 or 37°C. At the end of the experiment, the cells were fixed and processed for indirect immunofluorescence localization of the IgG. Photographs were taken and printed at a constant magnification of 1,800 $\times$ , and the number of fluorescent clusters (see Fig. 3) were tabulated from 12 different areas of each micrograph as described in Materials and Methods. The number of photographs analyzed for each experiment is shown in parenthesis.

\* Values are mean  $\pm$  SEM;  $t$  test of unpaired samples indicated  $p < 0.001$ .

meabilized before incubation with anti-folate receptor IgG. As shown in Fig. 5, there were not any vacuoles in the cell that bound IgG. The punctate staining was on the surface of the cell and appeared to have the same distribution as in cells incubated at 4°C with antibody (compare with Fig. 1 A). Some cells had a faint staining of the Golgi area, which indicates that the anti-folate receptor IgG was able to penetrate to the cell interior.

#### Ultrastructural Localization of Folate Receptor

Without the availability of a visible ligand, we had to rely on the anti-folate receptor IgG to localize receptor sites with the electron microscope. The fluorescence pattern indicated that the receptor was clustered; therefore, to obtain an overall view of the surface of cells we first localized anti-folate receptor binding sites in rapid-freeze, deep-etch replicas. With indirect immunogold labeling, the antibody binding sites were easily distinguished as clusters of gold particles distributed irregularly across the surface of the cell (Fig. 6 A). The clusters contained from 5 to 15 gold particles, had a variable shape, and were often associated with invaginations in the membrane (Fig. 6 A, arrows). Only a few unclustered gold particles were evident on cells incubated with nonimmune IgG (Fig. 6 B). Stereo images (Fig. 7) show in greater detail the clusters that were associated with invaginated regions of membrane (Fig. 7, A and B). Occasionally, the gold labeling circled the rim of an invaginated area (Fig. 7 A, open arrowhead); more commonly, the clusters were either in the vicinity of an invagination (Fig. 7, A and B, arrow), or over a flat segment of membrane (Fig. 7 B, solid arrowhead). The average area occupied by a cluster of gold particles was calculated to be 0.023  $\mu\text{m}^2$ .

We next examined thin sections of cells that had been incubated at either 4°C (Fig. 8 A) or 37°C (Fig. 8 C) with anti-receptor IgG before chilling to 4°C and processing for indirect immunogold labeling before fixation. As in the freeze-etch replicas, gold particles were highly clustered on the surface, regardless of the incubation temperature (compare Fig. 8, A and C), and many of the clusters were associated with uncoated pits (Fig. 8 C, inset). Both the amount of immunogold that was clustered (82% at 4°C; 86% at 37°C) and the density of gold in a cluster (6.3 parti-

cles/clusters at 4°C; 6.2 particles/cluster at 37°C) were not affected by temperature (Table II). On the other hand, the cells incubated at 37°C had 1.33 times more clusters than the cells incubated at 4°C (Table II). There was negligible labeling when cells were incubated at 4°C with nonimmune IgG (Fig. 8 B).

To determine if receptor clusters were associated with any membrane specialization, we quantitatively evaluated the distribution of gold clusters (Table II). The results of Fig. 4 indicated that the anti-folate receptor IgG was not internalized by clathrin-coated pits. Interestingly, we detected a weak association of anti-receptor IgG-gold clusters with coated pits in 4°C incubated cells (2.5% of clusters over 0.7% of surface), but in 37°C incubated cells there was no association of clusters with this membrane specialization (0.5% of clusters over 0.5% of surface). Contrasted with coated pits, there was a marked association of clusters with uncoated pits at both incubation temperatures (18.9% over 1.2–1.5% of surface). Moreover, 39–44% of the uncoated pits were labeled.

We also fixed and permeabilized cells (Fig. 8 D) to localize receptors at internal sites. After permeabilization with Tween-20 and incubation with antibody at 4°C, gold particles were found in clusters at the cell surface, but endosomes and lysosomes (Fig. 8 D, curved arrow) were devoid of label. The permeabilization treatment combined with immunogold labeling made it difficult to identify uncoated pits. We did not find any gold clusters on the basal or lateral surfaces of the cells, which agrees with the immunofluorescence images that show receptors are only at the apical surface.

#### Discussion

The folate receptor mediates the uptake of 5-methyltetrahydrofolic acid in folate-depleted tissue culture cells. Evidence is mounting that this receptor functions to concentrate 5-CH<sub>3</sub>FH<sub>4</sub> at the cell surface so that the vitamin can be efficiently transferred into the cell cytoplasm (28). To understand how this membrane protein performs this task, the anatomical organization of the receptor in cells where it is known to be active must be determined.

By both immunofluorescence and immunoelectron microscopy, the receptor was found to be clustered on the surface of MA104 cells, as well as on other cells that were examined. Every effort was made to rule out the possibility that the antibody induced receptor clustering; even cells that were prefixed, permeabilized, and incubated with both primary and secondary antibodies at 4°C had clustered receptors (Fig. 8 D). Moreover, when cells were incubated with anti-folate receptor IgG at 37°C, the size of the cluster remained the same as at 4°C, which indicates that higher order aggregates were not induced by the antibody at temperatures where the membrane is more fluid.

When the cells were incubated with antibody at 4°C, there was an average of 1.0 cluster/ $\mu\text{m}^2$  of the membrane. These cells bind 1 pmol/10<sup>6</sup> cells of 5-methyl[<sup>3</sup>H]tetrahydrofolic acid at 4°C (27), which equals 600,000 receptors exposed at the surface of each cell. Since we only found receptors on the apical surface and the number of clusters was  $\sim$ 800/cell, then each cluster contains  $\sim$ 750 receptors. The area occupied by a cluster was calculated from rapid-freeze, deep-

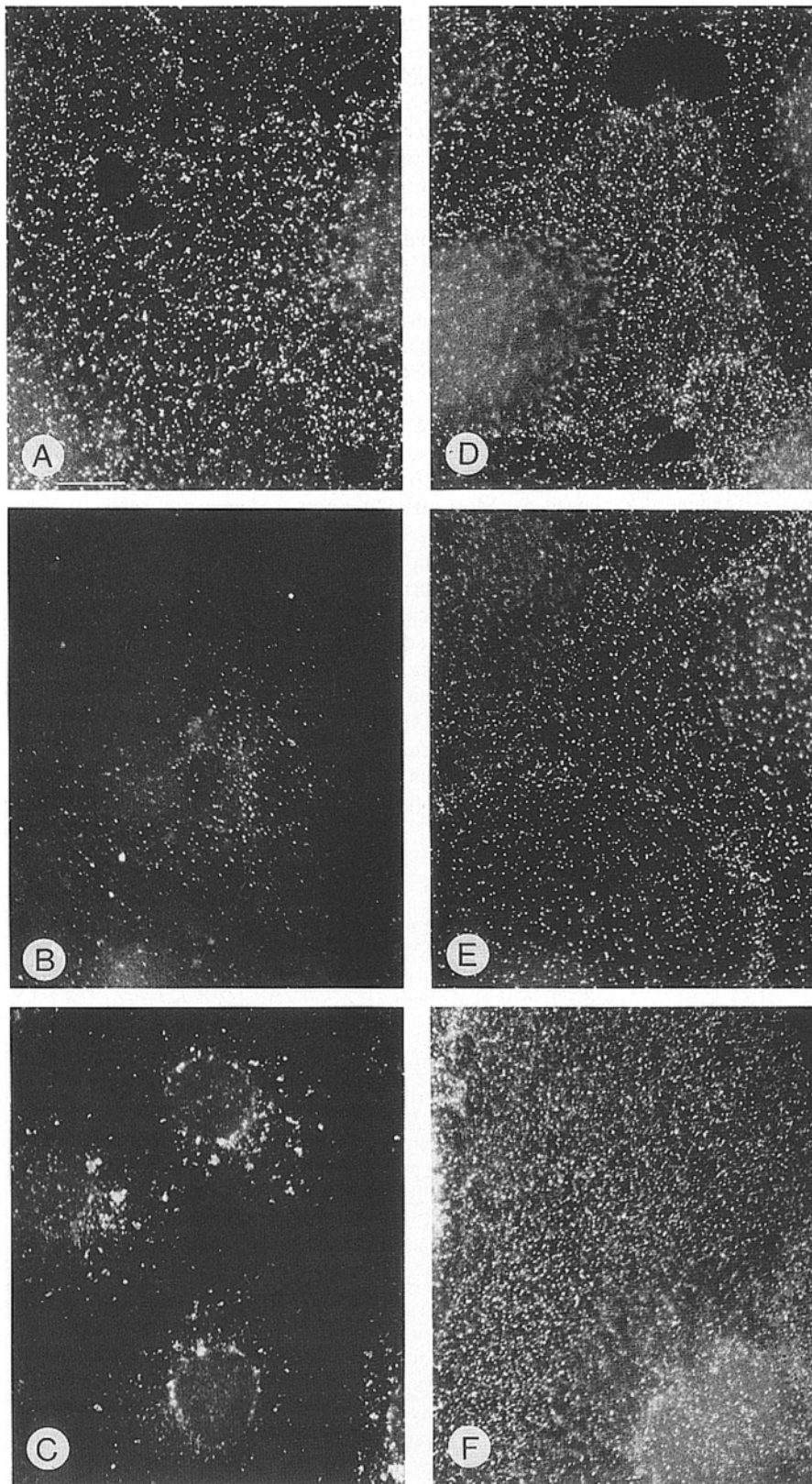


**Figure 4.** Internalization of anti-LDL receptor IgG (A-C) but not anti-folate receptor IgG (D-F) at 37°C. MA104 cells were grown in lipoprotein-deficient serum, chilled to 4°C, and incubated with either 40  $\mu\text{g}/\text{ml}$  of anti-LDL receptor IgG (A-C) or 17  $\mu\text{g}/\text{ml}$  of anti-folate receptor IgG (D-F) for 1 h. Cells were washed and either fixed (A and D) or warmed to 37°C for 30 min (B, C, E, and F) before fixation. One set of the warmed cells (C and F) was permeabilized, and the other set (B and E) was processed without permeabilization. After the respective treatments, each set of cells was processed for indirect immunofluorescence localization of the respective IgG. Bar, 10  $\mu\text{m}$ .

etch images and found to be 0.023  $\mu\text{m}^2$ , which gives an average receptor density within a cluster of  $\sim 32,000/\mu\text{m}^2$ . For comparison, the density of rhodopsin in rod outer segment membrane is  $\sim 20,000/\mu\text{m}^2$  (15), 3-hydroxy-3-methyl-

glutaryl-coenzyme A reductase in smooth endoplasmic reticulum membrane is  $\sim 700/\mu\text{m}^2$  (7), and the LDL receptor in coated pits is  $\sim 600/\mu\text{m}^2$  (Anderson, R. G. W., unpublished calculations). Quinn et al. (41) used 50,000 D as an

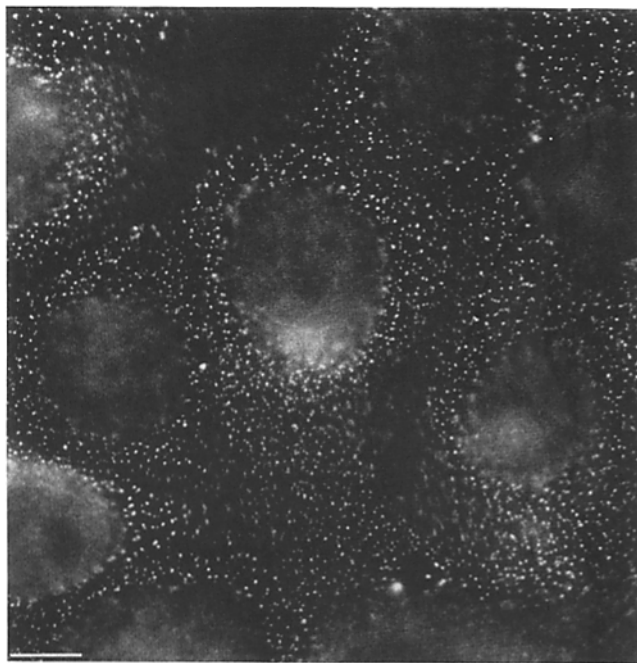


**Figure 5.** Immunofluorescence localization of the folate receptor in fixed and permeabilized cells. MA104 cells were fixed, permeabilized with Tween-20, and incubated with 17  $\mu\text{g/ml}$  of anti-folate receptor IgG for 1 h at 4°C. Cells were then incubated with 25  $\mu\text{g/ml}$  of fluorescein-labeled goat anti-chicken IgG for 1 h at 4°C. Bar, 9  $\mu\text{m}$ .

average size for a membrane protein and calculated that in the plasma membrane of cells the protein density is 30,000 molecules/ $\mu\text{m}^2$ . Therefore, within each cluster the density of folate receptor molecules may be high enough to exclude other membrane proteins; moreover, the fatty acids of the folate receptor GPI anchor probably influence the properties of the lipid bilayer within the cluster.

Previous studies have shown that, when MA104 cells are incubated with radiolabeled folic acid at 37°C for 1 h, the membrane binds  $\sim 1.7$  times more ligand than when incubated for the same time at 4°C (27), apparently owing to the exposure of more receptor to the ligand at the higher temperature. When 37°C incubated cells are chilled to 4°C and subjected to an acid wash, 50% of the folic acid is released; all of the label is released from cells incubated only at 4°C. These and other experiments indicate that the receptor recycles (27, 28). The recycling could be cyclic transformation from an active to an inactive conformation without a change in topological orientation at the cell surface. Alternatively, the receptor recycles by moving in and out of the cell. Our finding that cells incubated with anti-receptor IgG at 37°C for 1 h had 1.6 times more fluorescent foci than cells exposed to the antibody at 4°C suggests that the receptors physically move from an inaccessible to an accessible location at 37°C, which is consistent with vesicular movement of the receptor.

We detected quantal receptor movement at 37°C. Greater than 80% of the immunogold label was clustered at 4°C and neither the size of the clusters nor the number of immunogold particles per cluster was increased at 37°C. As judged by both immunofluorescence and immunoelectron microscopy, however, the number of clusters was signifi-

cantly increased at 37°C. Since there was no evidence that the antibody induced receptor clustering, each cluster appears to behave like a unit of receptors that move in and out of the cell.

The electron microscopy studies were designed to look for a vesicle system that carries the receptor through its recycling itinerary because we think that it is unlikely that a GPI-linked membrane protein would become inaccessible by flipping from the outside surface of the lipid bilayer to the inside surface. Originally, the clathrin-coated pit pathway was a candidate. The results, however, appear to rule out this possibility: (a) receptors were weakly associated with coated pits at 4°C but not at 37°C; (b) whereas MA104 cells would internalize anti-LDL receptor IgG, cells incubated at 37°C with anti-folate receptor IgG did not internalize the antibody into lysosomes; and (c) when the cells were fixed and permeabilized to examine the location of intracellular receptors, we found no evidence for receptors in endosomes or lysosomes, even though a variable amount of receptor was seen in the Golgi region. These results imply that the bulk of the receptors are closely associated with the cell surface membrane, which is consistent with cell fractionation studies that showed that all of the receptors migrate on Percoll gradients with a single plasma membrane fraction (27).

Both rapid-freeze, deep-etch images and thin section images of anti-folate receptor IgG gold labeling experiments showed that many of the receptor clusters were associated with a noncoated, invaginated region of membrane. Occasionally, receptors appeared to be physically within the invaginated region (Fig. 7 A), but more often label was nearby the invagination. Despite numerous attempts, we were unable to detect by electron microscopy movement of bound antibody into a vesicle at 37°C.

If the invaginations correspond to nascent vesicles that are capable of internalizing the receptor clusters, then using electron microscopic immunocytochemistry we should be able to detect receptors in vesicles that originate from these invaginations. Despite an enormous amount of effort, we have not been able to demonstrate the presence of receptor in a vesicle. Regardless of the sequence of antibody addition or the fixation/permeabilization protocol, we failed to find a receptor-positive vesicle. Therefore, either the receptor-positive vesicles do not exist or the conditions for doing the immunocytochemistry alter the receptor distribution as well as the morphology of the vesicles.

The noncoated invaginations morphologically resemble caveolae (1, 3, 12–14, 20, 46). Caveolae (also called plasmalemmal vesicles [44, 45]) are membrane specializations that are widely distributed among cells but are most numerous in endothelial and smooth muscle cells (1, 44). Their precise function is unknown: some evidence points towards an endocytic activity (21, 44, 45, 47), whereas other studies suggest that they are a permanent feature of the cell membrane (12, 14). Although in thin section electron microscopic images, caveolae are recognized by their size (60 nm diameter) and invaginated morphology, the inner surface of these regions of membrane has a distinctive coat material, which can only be seen in rapid-freeze, deep-etch replicas (3) or high resolution scanning microscopy images (40). The coat consists of evenly spaced filaments that are arranged into concentric whorls to form a “scroll-like” or “finger print-like” structure. These coated domains are either flat or

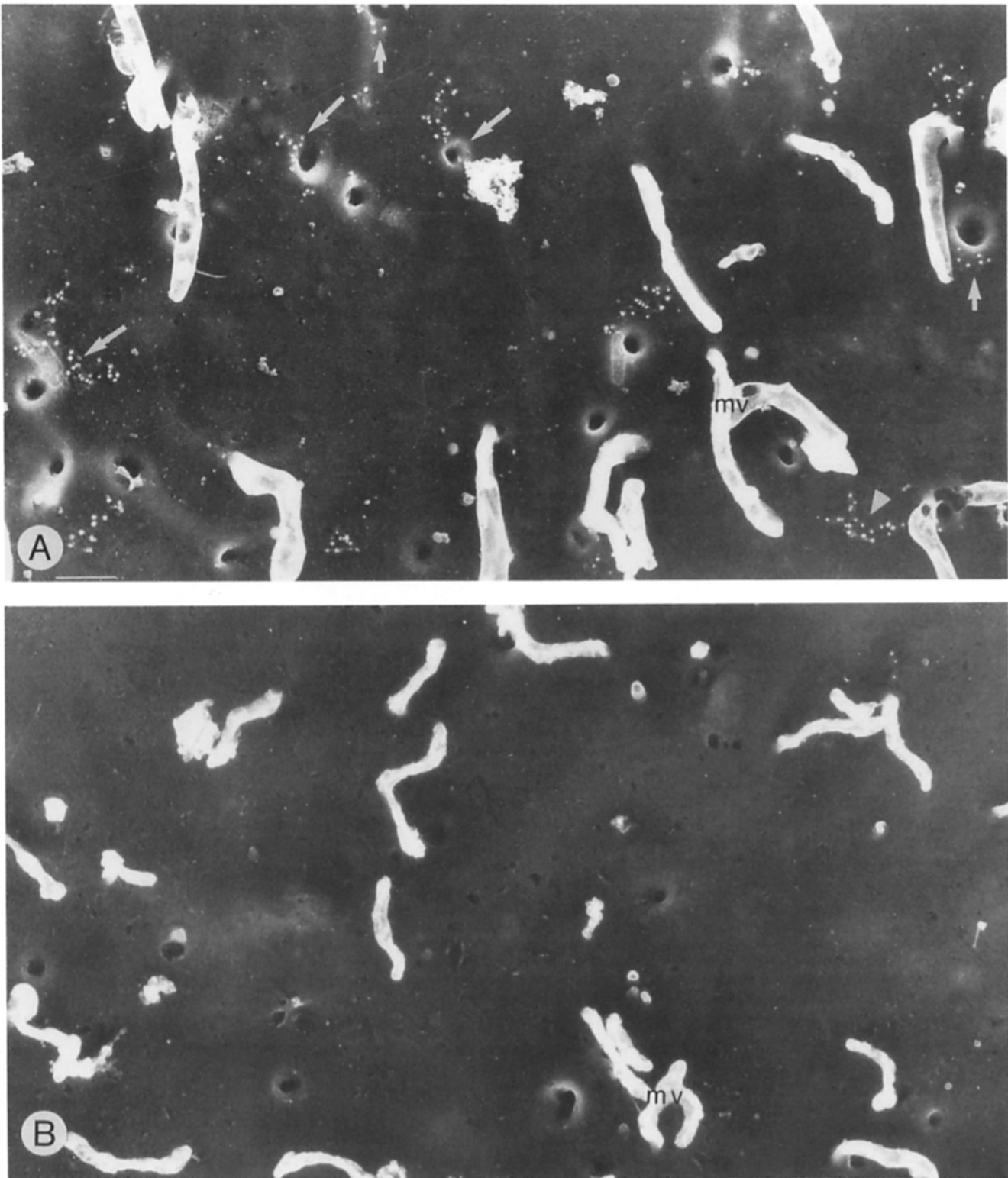


**Figure 6.** Immunogold localization of anti-folate receptor IgG binding sites in rapid-freeze, deep-etch replicas. MA104 cells were chilled to 4°C and incubated with either 42  $\mu\text{g}/\text{ml}$  of anti-folate receptor IgG (A) or nonimmune IgG (B) for 1 h at 4°C. The cells were washed and incubated with 25  $\mu\text{g}/\text{ml}$  of rabbit anti-chicken IgG for 1 h followed by a 1-h incubation with a 1:50 dilution of goat anti-rabbit IgG conjugated to gold (10 nm diameter), all at 4°C. The cells were fixed with 4% glutaraldehyde and processed for freeze-etching. Arrows indicate gold clusters near invaginations. Arrowhead indicates gold clusters on undifferentiated membrane. MV, microvilli. Bar, 0.3  $\mu\text{m}$ .

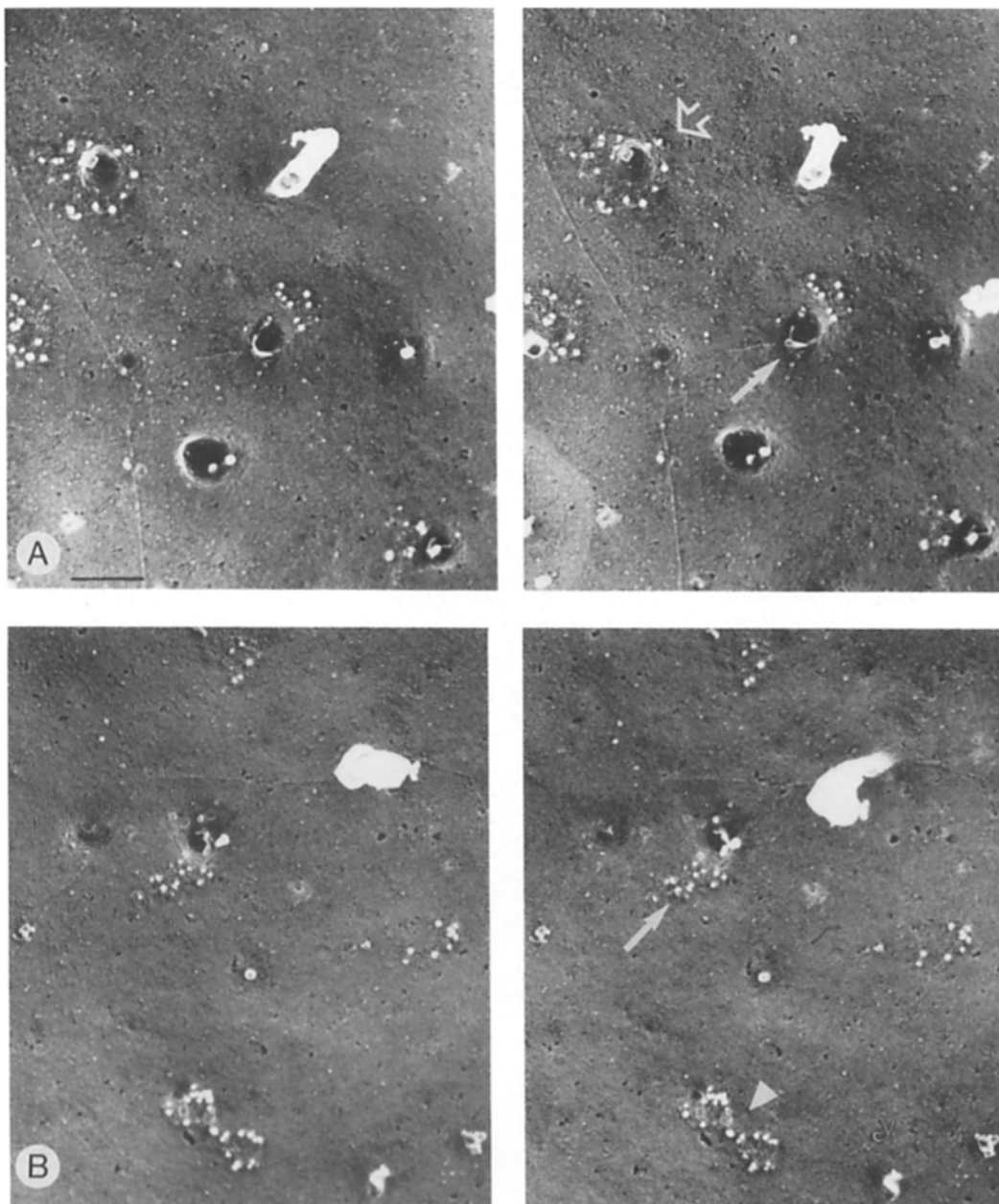


**Figure 7.** Stereo views of anti-receptor binding sites in rapid-freeze, deep-etch replicas. Samples were prepared as described in Fig. 7. Open arrow points to a gold cluster on the rim of an invagination. Solid arrow shows a gold cluster at the edge of an invagination. Arrowhead points to a gold cluster that is not near an invagination. Bar, 0.2  $\mu\text{m}$ .

highly curved, which suggests that the coat controls the curvature of the membrane.

Other membrane receptors that have been found to be associated with caveolae include those for albumin in endothelial cells (22), as well as cholera toxin and tetanus toxin in 3T3 L1 fibroblasts (38, 47). In addition, Ryan and Smith (43) showed that 5'-nucleotidase, another GPI-linked membrane protein (19), was associated with caveolae. Tran et al. (47) have quantified this association for cholera toxin-gold conjugates and find that 15–20% of the label is in uncoated pits that have the morphology of caveolae. They calculate an association index (percent of label associated with mem-

brane region divided by percent of cell surface occupied by membrane region) of 3.4–4.2. Approximately the same percent of the folate receptor clusters were associated with caveolae but we calculate an index of  $\sim 16$ , apparently because the MA104 cell surface contains fewer caveolae ( $\sim 1.5\%$  of surface) than 3T3 L1 cells. The association index we calculated may be less than the actual index because many of the gold clusters could have been associated with noninvaginated caveolae, which can only be detected in freeze-etch replicas by virtue of their characteristic coat material (3).

The caveolae may be the membrane specialization that mediates the delivery of 5- $\text{CH}_3\text{FH}_4$  to the cytoplasm of the

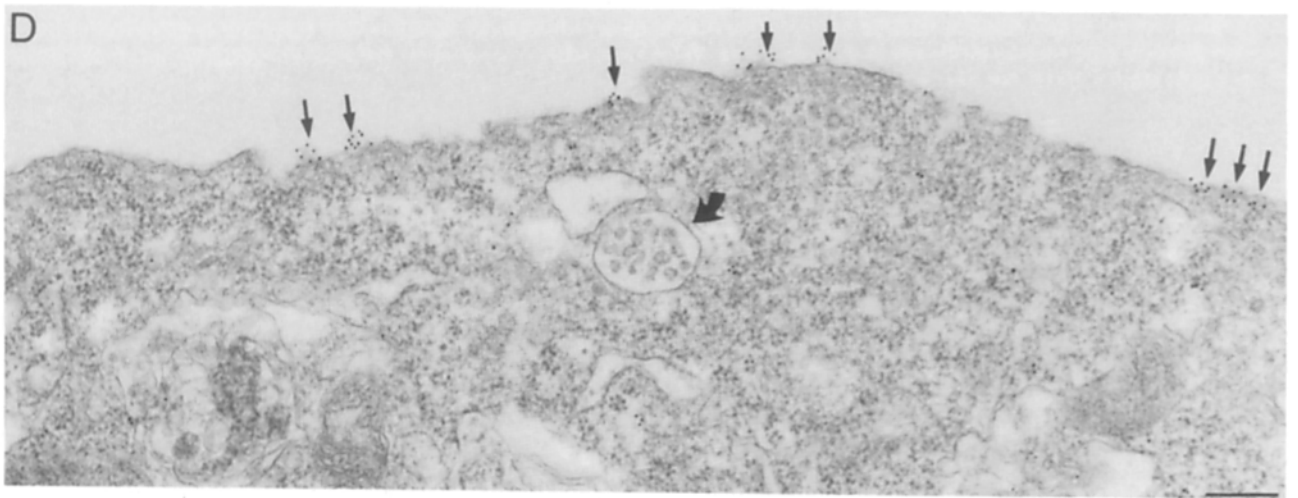
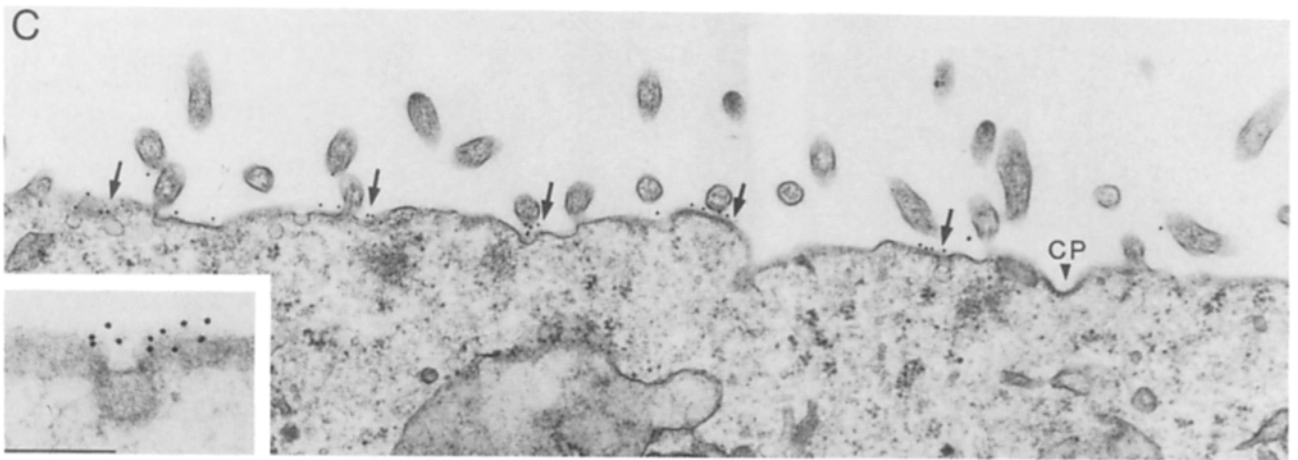
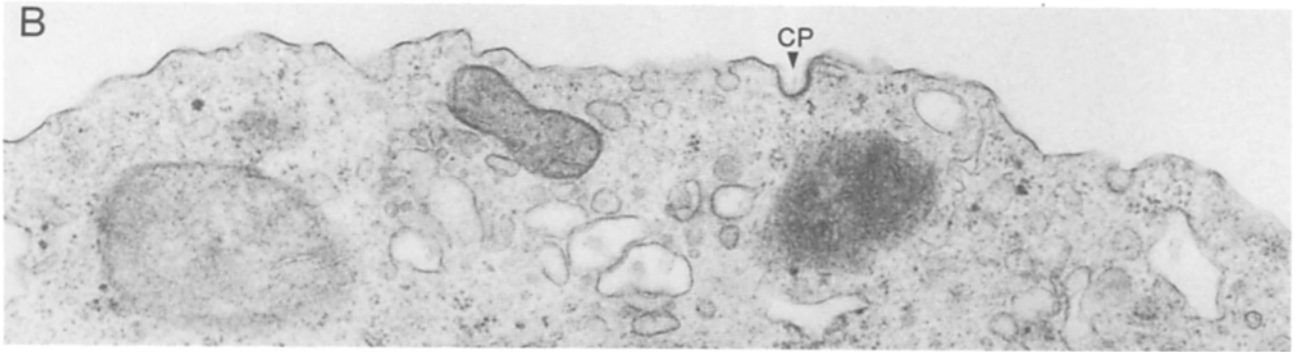
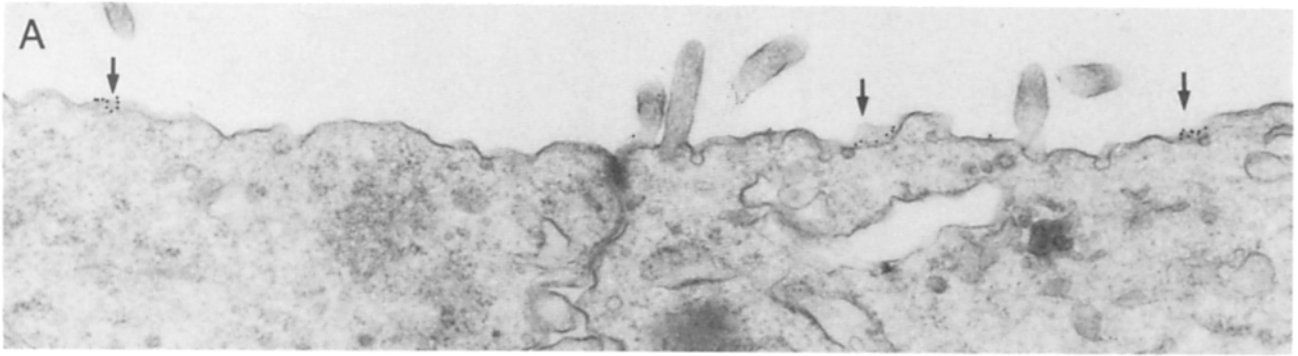


Table II. Quantitative Analysis of Anti-folate Receptor IgG Gold Clusters in MA104 Cells

Temperature	Gold clusters bound			Structures per 10 $\mu\text{m}$ of membrane			Surface that was uncoated pit	Surface that was coated pit	Uncoated pits labeled
	Coated pits	Uncoated pits	Undifferentiated membrane	Gold clusters	Uncoated pits	Coated pits			
$^{\circ}\text{C}$	%	%	%	No.	No.	No.	%	%	%
4	2.5	18.9	78.6	3.9	1.9	0.6	1.2	0.7	39
37	0.5	18.9	80.6	5.2	2.3	0.5	1.5	0.5	44

MA104 cells were incubated with 42  $\mu\text{g}/\text{ml}$  of anti-folate receptor IgG at the indicated temperature for 1 h. Cells were then chilled to 4 $^{\circ}\text{C}$  and processed for indirect immunogold localization of IgG binding sites before fixation. The data is the average of two separate experiments measuring a total of 1,112  $\mu\text{m}$  of membrane for each temperature. At 4 $^{\circ}\text{C}$ , 82% of the gold was clustered with an average of 6.3 gold particles/cluster. At 37 $^{\circ}\text{C}$ , 86% of the gold was clustered with an average of 6.2 gold particles/cluster. This analysis only pertains to clusters of gold where a cluster has more than three gold particles. The number of clusters per micrometer of membrane in nonimmune treated samples at both temperatures was below detection (Fig. 8 B).

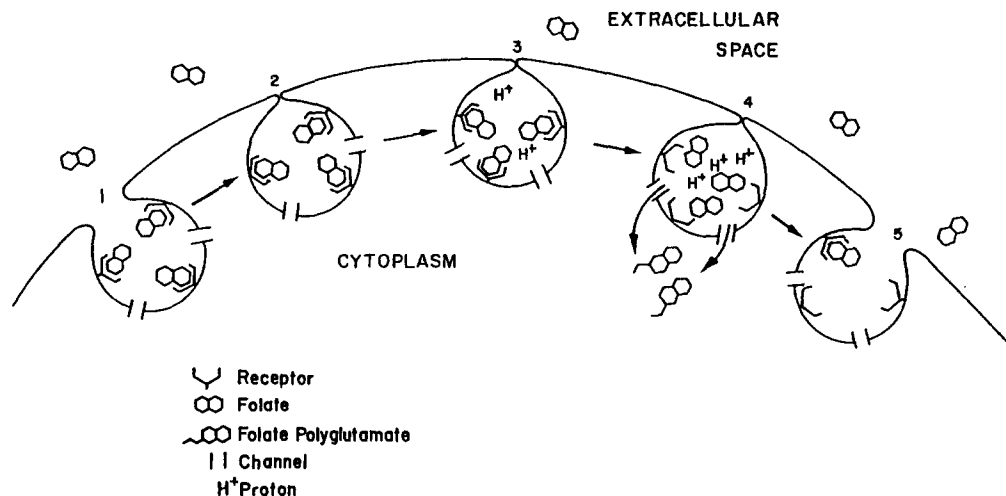


Figure 9. Receptor-coupled transmembrane transport: a model for how the caveolae might function as mediators of folate transport. See text for discussion.

cell. To account for the results from previous studies, we have suggested that the folate receptor functions to concentrate 5- $\text{CH}_3\text{FH}_4$  at the cell surface and deliver the vitamin to a vesicle (28). Subsequently, 5- $\text{CH}_3\text{FH}_4$  dissociates from the receptor at an acid pH and moves across the membrane into the cytoplasm, possibly by a folate-regulated transporter. Fig. 9 presents a model for how this process might occur within caveolae. The folate receptor is arranged in clusters on the cell surface in close proximity to a transmembrane transporter(s) (Fig. 9, 1). Both sets of molecules are located in caveolae, which are capable of transiently closing to form a membrane-bound compartment that protects the receptor both from acid treatment and from anti-folate receptor IgG (Fig. 9, 2). Once the caveolae is closed, the 5- $\text{CH}_3\text{FH}_4$  dissociates from the receptor, possibly as a result of acidification of the lumen (Fig. 9, 3). The 5- $\text{CH}_3\text{FH}_4$  then moves across the membrane via the transporter, using

the energy generated by the  $\text{H}^+$  gradient (Fig. 9, 4). When the 5- $\text{CH}_3\text{FH}_4$  reaches the cytoplasm, it is covalently modified by the addition of multiple glutamic acid residues. The folylpolyglutamate is unable to move back across the membrane, which traps the 5- $\text{CH}_3\text{FH}_4$  within the cytoplasm. Finally, the receptor containing caveolae unseals, which exposes the receptors for the next cycle (Fig. 9, 5).

The model does not require that the caveolae pinch off from the membrane. We invoke this condition because we have failed to find the receptor in an intracellular vesicle and because of the many detailed studies showing that caveolae appear to spend most of the time at the cell surface (12–14, 20). The caveolae may be specialized for transiently forming a closed compartment simply by repeated cycles of membrane invagination and evagination.

In conclusion, the folate receptor appears to represent a new class of membrane receptors that recycle while remain-

Figure 8. Immunogold localization of anti-folate receptor IgG binding sites before embedding (A–C) or after fixation and permeabilization (D). Cells were either incubated at 4 $^{\circ}\text{C}$  (A and B) or 37 $^{\circ}\text{C}$  (C) with IgG before processing as described in Fig. 6 and embedding in Eponate. Another set was fixed, permeabilized with Tween-20, and incubated with IgG followed by DNP-labeled goat anti-chicken IgG before embedding in Eponate (D). DNP was localized in thin sections by the method of Pathak and Anderson (39). A, C, and D were incubated with anti-folate receptor IgG, and B was incubated with nonimmune IgG. Bar: (A–D) 0.3  $\mu\text{m}$ ; (inset) 0.1  $\mu\text{m}$ .

ing tightly associated with the plasma membrane. The receptor is unusual in several respects. Unlike receptors that enter cells via coated pits, this receptor appears to be clustered independently of its association with any membrane specialization; even the receptors over undifferentiated membrane were clustered. The receptor cluster, rather than individual receptors, appears to recycle. Receptor clusters are associated with caveolae even though the receptor lacks a membrane-spanning region and a cytoplasmic tail. Future studies will hopefully elucidate the peculiar behavior of this receptor and clarify how caveolae are involved in 5-CH<sub>3</sub>-FH<sub>4</sub> delivery to the cytoplasm of cells.

We would like to thank William C. Donzell for the preparation of the rapid-freeze, deep-etch replicas and photographs and Ms. Anita Streckfuss and Dr. Jeff Zweiner for isolation of the folate receptor from placental tissue. We would also like to thank Ms. Mary Surovik and Ms. Yvonne Jones for patiently typing the manuscript.

The work was supported by grant HL20948 from the National Institutes of Health, grant CH228 from the American Cancer Society, and the King Foundation. B. A. Kamen is a Burroughs Wellcome scholar.

Received for publication 20 July 1989 and in revised form 3 November 1989.

## References

- Anderson, R. G. W. 1981. Cell surface membrane structure and the function of endothelial cells. In *Structure and Function of the Circulation*. Vol. 3. C. J. Schwartz, N. T. Werthessen, and S. Wolf, editors. Plenum Publishing Corp., New York. 239-286.
- Anderson, R. G. W. 1986. Methods for visualization of the LDL pathway in cultured human fibroblasts. *Methods Enzymol.* 129:201-215.
- Anderson, R. G. W. 1990. Molecular motors that shape endocytic membrane. In *Intracellular Trafficking of Proteins*. C. J. Steer and J. Hanover, editors. Cambridge University Press, London. In press.
- Anderson, R. G. W., and J. Kaplan. 1983. Receptor-mediated endocytosis. In *Modern Cell Biology*. B. Satir, editor. Alan R. Liss, Inc., New York. 1-52.
- Anderson, R. G. W., J. L. Goldstein, and M. S. Brown. 1977. A mutation that impairs the ability of lipoprotein receptors to localize in coated pits on the cell surface of human fibroblasts. *Nature (Lond.)* 270:695-699.
- Anderson, R. G. W., M. S. Brown, U. Beisiegel, and J. L. Goldstein. 1982. Surface distribution and recycling of the LDL receptor as visualized with anti-receptor antibodies. *J. Cell Biol.* 93:523-531.
- Anderson, R. G. W., L. Orci, M. S. Brown, L. M. Garcia-Segura, and J. L. Goldstein. 1983. Ultrastructural analysis of crystalline endoplasmic reticulum in UT-1 cells and its disappearance in response to cholesterol. *J. Cell Sci.* 63:1-20.
- Antony, A. C., M. A. Kane, R. M. Portillo, P. C. Elwood, and J. F. Kolhouse. 1985. Studies of the role of a particulate folate-binding protein in the uptake of 5-methyltetrahydrofolate by cultured human KB cells. *J. Biol. Chem.* 260:14911-14917.
- Benedict, A. A. 1967. Production and purification of chicken immunoglobulins. In *Methods in Immunology and Immunochemistry*. C. A. Williams and M. W. Chase, editors. Academic Press, Inc., New York. 229-237.
- Bretscher, M. S., J. N. Thomson, and B. M. F. Pearse. 1980. Coated pits act as molecular filters. *Proc. Natl. Acad. Sci. USA* 77:4156-4159.
- Brown, M. S., R. G. W. Anderson, and J. L. Goldstein. 1983. Recycling receptors: the round trip itinerary of migrant membrane proteins. *Cell* 32:663-667.
- Bundgaard, M. 1983. Vesicular transport in capillary endothelium: does it occur? *Fed. Proc.* 42:2425-2430.
- Bundgaard, M., J. Frokjaer-Jensen, and C. Crone. 1979. Endothelial plasmalemmal vesicles as elements in a system of branching invaginations from the cell surface. *Proc. Natl. Acad. Sci. USA* 76:6439-6442.
- Bundgaard, M., P. Hagman, and C. Crone. 1983. The three-dimensional organization of plasmalemmal vesicular profiles in the endothelium of rat heart capillaries. *Microwasc. Res.* 25:358-368.
- Chen, Y. S., and W. L. Hubbell. 1973. Temperature and light dependent structural changes in rhodopsin-lipid membranes. *Exp. Eye Res.* 17:517-532.
- Davis, C. G., M. A. Lehrman, D. W. Russell, R. G. W. Anderson, M. S. Brown, and J. L. Goldstein. 1986. The J. D. mutation in familial hypercholesterolemia: amino acid substitution in cytoplasmic domain impedes internalization of LDL receptors. *Cell* 45:15-24.
- Davis, C. G., I. R. van Driel, D. W. Russell, M. S. Brown, and J. L. Goldstein. 1987. The low density lipoprotein receptor: identification of amino acids in cytoplasmic domain required for rapid endocytosis. *J. Biol. Chem.* 262:4075-4082.
- Elwood, P. C., M. A. Kane, R. M. Portillo, and J. F. Kolhouse. 1986. The isolation, characterization, and comparison of the membrane-associated and soluble folate-binding proteins from human KB cells. *J. Biol. Chem.* 261:15416-15423.
- Ferguson, M. A. J., and A. F. Williams. 1988. Cell-surface anchoring of proteins via glycosyl-phosphatidylinositol structures. *Annu. Rev. Biochem.* 57:285-320.
- Frokjaer-Jensen, J. 1980. Three-dimensional organization of plasmalemmal vesicles in endothelial cells: an analysis by serial sectioning of frog mesenteric capillaries. *J. Ultrastruct. Res.* 73:9-20.
- Gartung, C., N. Braulke, A. Hasilik, and K. von Figura. 1985. Internalization of blocking antibodies against mannose-6-phosphate specific receptors. *EMBO (Eur. Mol. Biol. Organ.) J.* 4:1725-1730.
- Ghitescu, L., A. Fixman, M. Simionescu, and N. Simionescu. 1986. Specific binding sites for albumin restricted to plasmalemmal vesicles of continuous capillary endothelium: receptor-mediated transcytosis. *J. Cell Biol.* 102:1304-1311.
- Goldstein, J. L., S. K. Basu, and M. S. Brown. 1983. Receptor-mediated endocytosis of LDL in cultured cells. *Methods Enzymol.* 98:241-260.
- Goldstein, J. L., M. S. Brown, R. G. W. Anderson, D. W. Russell, and W. J. Schneider. 1985. Receptor-mediated endocytosis: concepts emerging from the LDL receptor system. *Annu. Rev. Cell Biol.* 1:1-39.
- Heuser, J. E., and R. G. W. Anderson. 1989. Hypertonic media inhibits receptor mediated endocytosis by blocking clathrin-coated pit formation. *J. Cell Biol.* 108:389-400.
- Kamen, B. A., and A. Capdevila. 1986. Receptor-mediated folate accumulation is regulated by the cellular folate content. *Proc. Natl. Acad. Sci. USA* 83:5983-5987.
- Kamen, B. A., M.-T. Wang, A. J. Streckfuss, X. Peryea, and R. G. W. Anderson. 1988. Delivery of folates to the cytoplasm of MA104 cells is mediated by a surface membrane receptor that recycles. *J. Biol. Chem.* 263:13602-13609.
- Kamen, B. A., C. A. Johnson, M.-T. Wang, and R. G. W. Anderson. 1989. Regulation of the cytoplasmic accumulation of 5-methyltetrahydrofolate in MA104 cells is independent of folate receptor regulation. *J. Clin. Invest.* 84:1379-1386.
- Kolhouse, J. F., C. Utley, and R. H. Allen. 1980. Isolation and characterization of methylmalonyl-CoA mutase from human placenta. *J. Biol. Chem.* 255:2708-2712.
- Lacey, S. W., J. M. Sanders, K. G. Rothberg, R. G. W. Anderson, and B. A. Kamen. 1989. cDNA for the folate binding protein correctly predicts anchoring to the membrane by glycosyl-phosphatidylinositol. *J. Clin. Invest.* 84:715-720.
- Lazarovits, J., and M. Roth. 1988. A single amino acid change in the cytoplasmic domain allows the influenza virus hemagglutinin to be endocytosed through coated pits. *Cell* 53:743-752.
- Low, M. G., and P. W. Kincade. 1985. Phosphatidylinositol is the membrane-anchoring domain of the Thy-1 glycoprotein. *Nature (Lond.)* 318:62-64.
- Low, M. G., and A. R. Saltiel. 1988. Structural and functional roles of glycosyl-phosphatidylinositol in membranes. *Science (Wash. DC)* 239:268-275.
- Lowry, O. H., N. J. Rosebrough, A. L. Farr, and R. J. Randall. 1951. Protein measurement with the Folin phenol reagent. *J. Biol. Chem.* 193:265-276.
- McHugh, M., and Y.-C. Cheng. 1979. Demonstration of high affinity folate binder in human cell membranes and its characterization in cultured human KB cells. *J. Biol. Chem.* 254:11312-11318.
- Mellman, I., and H. Plutner. 1984. Internalization and degradation of macrophage Fc receptors bound to polyvalent immune complexes. *J. Cell Biol.* 1170-1177.
- Mellman, I., H. Plutner, and P. Ukkonen. 1984. Internalization and rapid recycling of macrophage Fc receptors tagged with monovalent anti-receptor antibody: possible role of a prelysosomal compartment. *J. Cell Biol.* 98:1163-1169.
- Montesano, R., J. Roth, A. Robert, and L. Orci. 1982. Non-coated membrane invaginations are involved in binding and internalization of cholera and tetanus toxins. *Nature (Lond.)* 296:651-653.
- Pathak, R. K., and R. G. W. Anderson. 1989. The use of dinitrophenol-IgG conjugates to detect sparse antigens by immunogold labeling. *J. Histochem. Cytochem.* 37:69-74.
- Peters, K.-R., W. W. Carley, and G. E. Palade. 1985. Endothelial plasmalemmal vesicles have a characteristic striped bipolar surface structure. *J. Cell Biol.* 101:2233-2238.
- Quinn, P., G. Griffiths, and G. Warren. 1984. Density of newly synthesized plasma membrane proteins in intracellular membranes. II. Biochemical studies. *J. Cell Biol.* 98:2142-2147.
- Roth, M. G., C. Doyle, J. Sambrook, and M.-J. Gething. 1986. Heterologous transmembrane and cytoplasmic domains direct functional chimeric influenza virus hemagglutinins into the endocytic pathway. *J. Cell Biol.* 102:1271-1283.
- Ryan, J. W., and U. Smith. 1971. A rapid, simple method for isolating

- pinocytotic vesicles and plasma membrane of lung. *Biochim. Biophys. Acta.* 249:177-180.
44. Simionescu, N. 1983. Cellular aspects of transcapillary exchange. *Physiol. Rev.* 3:1536-1560.
45. Simionescu, N., M. Simionescu, and G. E. Palade. 1975. Permeability of muscle capillaries to small heme-peptides: evidence for the existence of patent transendothelial channels. *J. Cell Biol.* 64:586-607.
46. Somlyo, A. P., C. E. Devine, A. V. Somlyo, and S. R. North. 1971. Sarcoplasmic reticulum and the temperature-dependent contraction of smooth muscle in calcium-free solutions. *J. Cell Biol.* 51:722-741.
47. Tran, D., J.-L. Carpentier, F. Sawano, P. Gorden, and L. Orci. 1987. Ligands internalized through coated or noncoated invaginations follow a common intracellular pathway. *Proc. Natl. Acad. Sci. USA.* 84:7957-7961.